JOURNAL OF VIROLOGY, July 2007, p. 7435–7448 Vol. 81, No. 14
0022-538X/07/$08.00+0 doi:10.1128/JVI.00571-07

Bovine Papillomavirus Type 1 Infection Is Mediated by SNARE Syntaxin 18▽

Valerie Laniosz,[1] Kha C. Nguyen,[2] and Patricio I. Meneses[1,2]*

School of Graduate and Postdoctoral Studies,[1] and Department of Microbiology and Immunology, H. M. Bligh Cancer Research Laboratory, Chicago Medical School,[2] Rosalind Franklin University of Medicine and Science, North Chicago, Illinois 60064

Received 19 March 2007/Accepted 24 April 2007

Events that lead to viral infections include the binding of the virus to the target cells, internalization of the virus into the cells, and the ability of the viral genome to be expressed. These steps are mediated by cellular and viral proteins and are temporally regulated. The papillomavirus capsid consists of two virally encoded capsid proteins, L1 and L2. Much is known about the role of the major capsid protein L1 compared to what is known of the role of the L2 protein. We identified the interaction of the L2 protein with SNARE protein syntaxin 18, which mediates the trafficking of vesicles and their cargo between the endoplasmic reticulum, the *cis*-Golgi compartment, and possibly the plasma membrane. Mutations of L2 residues 41 to 44 prevented the interaction of L2 protein with syntaxin 18 in cotransfection experiments and resulted in noninfectious pseudovirions. In this paper, we describe that syntaxin 18 colocalizes with infectious bovine papillomavirus type 1 (BPV1) pseudovirions during infection but does not colocalize with the noninfectious BPV1 pseudovirions made with an L2 mutant at residues 41 to 44. We show that an antibody against BPV1 L2 residues 36 to 49 (αL2 36–49) binds to in vitro-generated BPV1 pseudoviral capsids and does not coimmunoprecipitate syntaxin 18- and BPV1 L2-transfected proteins. αL2 36–49 was able to partially or completely neutralize infection of BPV1 pseudovirions and genuine virions. These results support the dependence of syntaxin 18 during BPV1 infection and the ability to interfere with infection by targeting the L2-syntaxin 18 interaction and further define the infectious route of BPV1 mediated by the L2 protein.

Papillomaviruses (PVs) induce a variety of lesions such as cutaneous or genital warts in humans and exophytic papillomas of cutaneous or mucosal epithelia in animals. Human PV (HPV) infection is the most common sexually transmitted disease in the United States (approximately 5.5 million cases per annum) (31), and specific HPV genotypes (high risk) are the etiologic agents of cervical carcinoma, a major killer of women worldwide (23, 37–39). Bovine PV (BPV) infection causes benign tumors, which can result in squamous cell carcinoma in the presence of environmental factors such as bracken (7).

The PV capsids consist primarily of two virally encoded proteins, L1 and L2, at an estimated ratio of 30:1 (17, 49). The L1/L2 ratio suggests that there is one L2 at each of 12 capsid vertices (49). Each viral particle contains a single double-stranded circular DNA genome of about 8 kb bound by histone proteins (15, 24), and the virus is assembled in the nucleus of squamous epithelial cells into particles that are 52 to 55 nm in diameter (9).

The expression of the viral L1 protein in the absence of other viral proteins results in the packaging of viral DNA at inefficient levels (5, 50). The addition of L2 to viral particle production increases DNA packaging into virions (28, 53) and contributes to the infectious process of the virus (2, 18). Antibodies to L2 have proven to be neutralizing and have led to the finding that a portion of L2 is exposed on the capsid surface (8, 22, 29, 32, 42). By using antibodies to L2, it has been possible to show by electron microscopy (EM) that residues 61 to 83 and 116 to 123 of BPV type 1 (BPV1) L2 are exposed on the outer surface of viral particles (32). It has also been suggested by enzyme-linked pseudovirion capture assay using an L2 antibody that HPV type 16 residues 14 to 144 and in particular residues 32 to 81 are likely to reside on the surface of the viral capsid (30). These EM and neutralization data have led to several studies addressing the use of papillomavirus L2 sequences as vaccine targets for specific and multiple PV genotypes since the regions of L2 shown to be exposed on the capsid surface are more conserved than the loops of the L1 protein (29, 30, 36, 43, 48). In addition, there is evidence that upon cell binding, a conformational change allows for the exposure of hidden L2 residues that can serve as neutralizing epitopes (41, 46, 52). These latter experiments support the hypothesis that L2 is in part mediating the process of infection after viral binding to the cell surface, including the translocation of the encapsidated genome to the nucleus (1, 11, 18).

Recent improvements in the process to generate PV particles have made it possible to study the process of viral entry and infection in detail (4, 40). These pseudovirions are capable of encapsidating plasmid DNA containing transgenes and full papillomavirus genomes. The pseudovirion production methods rely on the formation of DNA-containing capsids in the artificial environment of the transformed cell line 293TT (4). The resulting viral particles are not fully matured until an overnight incubation at 37°C in which L1 disulfide bonds are made (4, 5, 41), although the particles are still infectious (6). It has been demonstrated that the addition of DNA into PV capsids causes a change in viral morphology since it confers a necessity for a second receptor for internalization (46), and

* Corresponding author. Mailing address: 3333 Green Bay Road, 2.351, Department of Microbiology and Immunology, Rosalind Franklin University of Medicine and Science, North Chicago, IL 60064. Phone: (847) 578-3000, ext. 7775. Fax: (847) 578-3349. E-mail: patricio.meneses@rosalindfranklin.edu.

▽ Published ahead of print on 2 May 2007.

DNA encapsidation renders the virions less susceptible to protease digestion, again suggesting that a tighter capsid is created (19). These in vitro-generated pseudovirions have been used to study viral infection and neutralization and dendritic cell activation and have been used in studies dealing with the role of nuclear compartments, known as ND10s, and cellular proteins such as dynein and syntaxin 18 (2, 12, 20, 21, 30). In addition, pseudovirions containing the cottontail rabbit PV genome that were generated in this fashion were recently shown to be infectious in vivo, and papillomatous growths were induced (10). Those studies suggest that the current strategy of pseudovirion production in 293TT cells results in biology analogous to that of genuine infectious virus particles.

In a previous study, we used a proteomics approach to identify L2 interacting cellular proteins (2). Our data showed the interaction of L2 with syntaxin 18, which has been found to be involved in endoplasmic reticulum (ER)-Golgi compartment trafficking of vesicles (26) and recently shown to play a role in phagocytosis (27). We identified that the region of L2 encompassing residues 41 to 44 was important for the interaction of BPV1 L2 protein with syntaxin 18 protein and is needed for infection. In the present study, we used an affinity-purified antibody to BPV1 L2 residues 36 to 49 to demonstrate that this region of L2 is exposed on viral particles after virus production and during infection. Using this antibody, we observed greater than 90% neutralization of infection by BPV1 pseudovirions and greater than 70% neutralization by genuine BPV1 virions. Our data show that this antibody interferes with both the coimmunoprecipitation of L2 with syntaxin 18 and the colocalization of pseudovirions with syntaxin 18, supporting the involvement of syntaxin 18 during infection.

MATERIALS AND METHODS

L2 peptides and antibodies. The following peptides were made (ADI, Dallas, TX): (i) WTP15L2 (CDTIADKILKFGGLA), corresponding to residues 36 to 49 of BPV1 L2, and (ii) SCR15L2 (CIDGLGKLATIDAKF), corresponding to the same BPV1 L2 residues in random order. The peptides were resuspended in serum-free Dulbecco's modified Eagle's medium (DMEM) at a 10 mM concentration. Antibodies to L2 residues 36 to 49 (referred to as αL2 36–49 in this paper) were made by ADI after conjugation of the 36- to 49-amino-acid peptide to keyhole limpet hemocyanin (KLH).

Pseudovirion production and purification. The bicistronic BPV1 L1 and L2 plasmid pShell, the green fluorescent protein (GFP) cDNA-containing packaging plasmid 8fwb, and the 293TT viral packaging cell line were a generous gift from P. M. Day and J. T. Schiller (4). Pseudovirion production and titer analysis were performed as described previously (4) (http://home.ccr.cancer.gov/lco/default.asp). Two Optiprep purifications were performed on the virus preparations used for EM studies.

Affinity purification of L2 peptide antibody. Affinity purification of antibody derived from the rabbits immunized with the BPV1 L2 peptide corresponding to residues 36 to 49 was performed using a Hi-trap NHS column (GE Healthcare, Piscataway, NJ). Once ligand-peptide was bound according to the manufacturer's instructions, 10 ml of immune serum diluted in 15 ml of phosphate-buffered saline (PBS) was circulated through the column for a period of 6 h on ice. The column was then washed with 20 volumes of ice-cold PBS. Bound antibody was eluted from the column using elution buffer (50 mM glycine, 150 mM NaCl) at pH 2.5, and fractions were neutralized to pH 7 using a 1/10 volume of 1.0 mM Tris (pH 7.5). Bicinchoninic acid protein assays were performed to determine the peak elution fraction and to determine the concentration of purified immunoglobulin G (Pierce, Rockford, IL). Western blots were used to determine that L2-specific antibody was purified.

Western blots. COS-7 cells were transfected using Lipofectamine 2000 according to the manufacturer's instructions (Invitrogen, Carlsbad, CA). Cells were harvested in ice-cold radioimmunoprecipitation assay buffer (1% sodium deoxycholate, 0.1% sodium dodecyl sulfate, 1% Triton X-100, 1% bovine hemoglobin, 1 mM iodoacetamide, 10 mM Tris HCl [pH 8.0], 140 mM NaCl, 0.025% NaN_3) containing protease inhibitors (GE Healthcare). Samples were run on a 10% sodium dodecyl sulfate-polyacrylamide gel as described previously (2). The anti-L2 antibody BL2 (a gift from Richard Roden, John Hopkins University, MD), anti-actin (Sigma), αL2 36–49, M2 FLAG (Sigma), and the anti-L1 antibody 1-H8 (GeneTex, San Antonio, TX) were used for Western analysis at a 1:1,000 dilution. Fluorescent secondary antibodies were used at 1:20,000 dilutions for 30 min at room temperature. Blots were scanned using the Odyssey imaging system (Li-Cor Inc., Lincoln, NE). Data were analyzed using software provided with the Odyssey system.

Neutralization experiments. In assays using immune and preimmune sera, the sera were diluted in DMEM–10% fetal bovine serum (DMEM-10) to 1/150, 1/60, and 1/30. These dilutions were incubated with BPV1 pseudovirions for 30 min at 37°C prior to their addition to 100,000 chilled (ice-cooled) cells/well on a 24-well plate. These infected cells were incubated on ice for 2 h and then washed with DMEM-10 two times to remove excess sera. Five hundred microliters/well of 37°C DMEM-10 was added, and the plates were incubated at 37°C in 5% CO_2 for 24 h. Infection levels were measured by fluorescence-activated cell sorter (FACS): 10,000 cells were counted by FACS, and the number of GFP-positive cells was used to determine percent infection. Assays using affinity-purified antibodies were carried out as described above except that antibodies were used at 2, 10, and 20 μg and preincubation of virus with antibody was done for an hour on ice. The infections in the presence of the affinity-purified antibody were allowed to proceed for up to 48 h.

Focus-forming assays. Focus-forming assays were done using a modification of a well-established protocol described previously by DiMaio (16) (D. DiMaio, Yale University, personal communication). In brief, C127 mouse fibroblasts were plated onto 60-mm^2 cell culture dishes at around 33% confluence and allowed to reach 75% confluence prior to infection with genuine BPV1 virions (ATCC, Manassas, VA). Twenty-four hours postinfection, cells were split 1:3 and kept at 37°C in 5% CO_2 for 2 weeks, with medium changes every 3 days. Cells were fixed with 70% isopropanol and stained with 1% methylene blue so that foci could be scored as described previously (45).

Immunofluorescence. Infected cells grown on glass coverslips (catalog number 12-545-80; Fisher Scientific, Piscataway, NJ) were fixed in 4% paraformaldehyde for 10 min at 4°C at the appropriate time points. Coverslips were treated as described previously (2). Working dilutions of the primary antibodies were as follows: rabbit anti-syntaxin 18 (a generous gift from M. Tagaya, Japan) was used at a 1:100 dilution, mouse anti-L1 antibody 5B6 hybridoma, which binds to fully formed viral particles and L1 pentamers (a gift from Richard Roden) was used at a 1:100 dilution, goat anti-EEA1 was used at a 1:100 dilution (Santa Cruz, Santa Cruz, CA), and goat anti-LAMP1 was used at a 1:100 dilution. EEA1 is a molecule found on early endosomes associated with Rab5 and with transferrin entry (34), a clathrin-mediated process of endocytosis (25); LAMP1 is a marker of the lysosomes and late endosomes (44). The fluorescently labeled Alexa Fluor secondary donkey anti-rabbit 488 antibody, donkey anti-mouse 594 antibodies, and chicken anti-goat 488 antibody were diluted to 1:2,000, and donkey anti-rabbit 647 antibody (Molecular Probes/Invitrogen, Eugene, OR) was diluted to 1:1,000. All antibodies were diluted in blocking buffer (0.2% fish skin gelatin, 0.2% Triton X-100, PBS). The nucleus was visualized using DAPI (4′,6′-diamidino-2-phenylindole) or TOPRO-3 (Invitrogen, Carlsbad, CA). Fluorescence confocal microscopy was performed with an Olympus Fluoview 300 microscope with Fluoview software (Olympus, Melville, NY) at the microscopy core of the Rosalind Franklin University of Medicine and Science.

Negative staining of viral particles for EM. Double-purified pseudovirions were bound to carbon-filmed nickel grids (Electron Microscopy Sciences, Hatfield, PA) by placing the grids face down onto a 20-μl drop of viral suspension for 15 min at room temperature, and the viral titer was $>5 \times 10^6$ infectious units/ml. After blocking (PBS, 5% bovine serum albumin, 5% rabbit serum, 5% mouse serum, 0.1% fish skin gelatin), grids were placed onto droplets containing either affinity-purified antibody αL2 36–49 and the hybridoma anti-L1 antibody 5B6 or affinity-purified glutathione *S*-transferase (GST) (ADI) as an isotypic control and 5B6 overnight at 4°C. Affinity-purified antibodies were used at 400 ng, and the hybridoma-derived 5B6 antibody was used at a 1:10 dilution in incubation buffer (PBS, 0.2% bovine serum albumin, 0.02% Na azide). After washing in incubation buffer, grids were floated on 20-μl droplets of secondary donkey anti-rabbit 6-nm-immunogold-labeled antibody and donkey anti-mouse 10-nm-immunogold-labeled antibody (Electron Microscopy Sciences) at a 1:20 dilution for 1 h at room temperature. Grids were washed extensively in incubation buffer and then fixed with 2% glutaraldehyde for 5 min, washed in incubation buffer, and negatively stained using 2% phosphotungstitic acid. Analysis was performed using a JEOL JEM-1230 transmission electron microscope at an accelerating velocity of 80 kV at the Rosalind Franklin University of Science and Medicine.

Other reagents. Syntaxin 18 constructs were provided by M. Tagaya (Tokyo University, Tokyo, Japan) and K. Hatsuzawa (Fukushima Medical University, Fukushima, Japan). M2 FLAG beads were purchased from Sigma. L2 mutant constructs were described previously (2). Control DNA vector control pA3M, a derivative of pCDNA3 (Invitrogen), was a gift from E. Robertson (University of Pennsylvania, Philadelphia, PA). DNA gel was stained with SYBR green (Molecular Probes/Invitrogen), and the GFP primers used for reverse transcription-PCR and PCR were obtained from Integrated DNA Technologies (Coralville, IA).

RESULTS

BPV1 L2 residues 41 to 44 are not involved in the formation of viral particles, DNA packaging, or initial viral entry but are necessary for infection. We previously demonstrated the coimmunoprecipitation and in vivo colocalization of wild-type BPV1 L2 (wtL2) protein and syntaxin 18, a resident protein of the ER (2). We showed that this interaction did not occur with BPV1 L2 protein that was mutated in residues 41 to 44 (L2ANS) and that pseudovirions generated with L2ANS were noninfectious. In order to understand the biological reason for the loss of infection using L2ANS, we reanalyzed the pseudovirions' ability to incorporate L2ANS, package DNA, and infect cells. As described previously (2), the L2ANS-purified pseudovirions had equivalent levels of L2 and L1 (Fig. 1 A) and an equivalent level of benzonase-resistant encapsidated DNA by real-time PCR: $1.39 \pm 0.18 \times 10^{10}$ for L2ANS and $1.77 \pm 0.31 \times 10^{10}$ for wtL2 (Fig. 1B) (the PCR sample is shown at cycle 35), and we observed no infection by FACS analysis with the L2ANS pseudovirions (Fig. 1C). Infection is measured as the number of GFP-transduced cells, since the encapsidated plasmid 8fwb has the GFP cDNA.

Since PV entry has been shown to occur primarily via clathrin-mediated endocytosis in which the pseudovirion staining overlaps with EEA1, an endosome marker involved in clathrin-mediated entry (25), and subsequently with the late endosome lysosome marker LAMP1 (3, 13, 44, 47, 51), we decided to compare the trafficking of wtL2 to that of defective L2ANS pseudoviral particles (Fig. 1D). The colocalizations of BPV1 pseudovirions stained with 5B6 (Fig. 1D, red arrows) and EEA1 (Fig. 1D, green arrows) or with LAMP1 (Fig. 1D, green arrows) were indistinguishable using either wtL2 (Fig. 1D, rows 1 and 3) or L2ANS (Fig. 1D, rows 2 and 4) pseudovirions (Fig. 1D, merged images). *z* stacks are shown to support the overlap in fluorescence from multiple viewing planes. This assay was performed with the hybridoma antibody 5B6, which recognizes L1 in intact L1 pseudoviral particles and in L1/L2 pseudoviral particles. Although our virion particle analysis shown in Fig. 1 confirms that the pseudoviral particles contain L2 and packaged DNA, we cannot exclude that there may be some L1-only pseudoviral particles. Studies have shown that the initial entry of L1 and L1/L2 particles is identical (46) and that L1-only pseudoviral particles are very poor at packaging DNA compared to L1/L2 pseudovirions (5, 50). Thus, these data demonstrate that although BPV1 pseudovirions made with L2ANS are similar to wtL2 pseudovirions in their capsid viral contents, abilities to package DNA, and initial entry into the endocytic pathway, they are noninfectious.

BPV1 pseudovirion interaction with syntaxin 18 during infection. Although we previously identified that a dominant negative syntaxin 18 disrupted BPV1 pseudovirion infections and that mutation of L2 residues 41 to 44 resulted in a loss of the interaction of L2-transfected protein with syntaxin 18 as well as a loss of infection (2), we had not addressed if there was a relationship between syntaxin 18 and infecting pseudovirions. The role of syntaxin 18 has been defined as an intracellular vesicle mover that can associate with EEA1 (27). In this study, we used confocal microscopy to address if syntaxin 18 interacted with wtL2- and/or L2ANS-generated BPV1 pseudovirions during infection (Fig. 2). Staining for endogenous syntaxin 18 (Fig. 2A, D, and G) in COS-7 cells that were infected with wtL2 pseudovirions (BPV1 wtL2) (Fig. 2A to C1) and pseudovirions with anti-L1 5B6 demonstrates the overlap of infectious wtL2 pseudovirions and syntaxin 18 (Fig. 2C and C1, yellow arrow) at 4 h. In contrast, the staining for endogenous syntaxin 18 and the noninfectious L2ANS pseudovirions (BPV1 L2ANS) does not overlap at 4 h (Fig. 2D to F1) or even after 24 h (Fig. 2G to I1). Syntaxin 18 has also been identified as being an ER marker (26). We used a second ER marker, calnexin (Fig. 2J and M), to confirm the results of our colocalization analysis. Cells infected with and stained for wtL2 pseudovirions (Fig. 2K) demonstrated overlap with calnexin at 4 h (Fig. 2L and L1), whereas cells infected with BPV1 L2ANS (Fig. 2N) do not show colocalization between the mutant virus and calnexin at 4 h (Fig. 2O and O1).

It has recently been described that syntaxin 18 is involved in the process of phagocytosis (27). Hatsuzawa et al. confirmed the role of syntaxin 18 using a fusion of a derivative of GFP called VENUS to syntaxin 18 (VENUS syn 18). We transfected COS-7 cells with 500 ng of VENUS syn 18 in order to further analyze the interaction of syntaxin 18 with PV pseudovirions (Fig. 2P to X1). In these experiments, VENUS syn 18 was transfected 12 h before viral infections in order to allow for its expression. We observed the overlap of VENUS syn 18 with the wtL2 pseudovirions at 4 h (Fig. 2I and I1), demonstrating a similar signal overlap as was observed with the staining for endogenous syntaxin 18 and calnexin. Infection with BPV1 L2ANS mutant pseudovirions (Fig. 2V) displayed a lack of overlap between 5B6 and VENUS syn 18 at 4 h (Fig. 2U, merge) and 24 h (Fig. 2X, merge). Although we observed continued staining of L2ANS pseudovirions using 5B6, none was observed for wtL2 pseudovirions past 6 h (data not shown). These data demonstrate that infectious pseudovirions interact with syntaxin 18 during infection and that the noninfectious pseudovirions made with L2 residues 41 to 44 do not overlap with syntaxin 18.

Production of BPV1 L2 antibodies using synthetic peptide corresponding to residues 36 to 49. Our data showed that capsids made with L2 mutated at residues 41 to 44 were noninfectious. We wanted to address if this epitope could be neutralizing and used as a tool to understand and define the infectious BPV1 pathway further. We generated antibodies to a peptide corresponding to BPV1 L2 residues 36 to 49 (Fig. 3A) conjugated to KLH by the addition of a cysteine at the N terminus of the peptide. To determine the antibody's specificity of L2 binding, BPV1 L2 lysates corresponding to full-length L2 and L2 deletion mutants described previously (2) were made from transfected COS-7 cells. Figure 3B depicts the 469 residues of BPV1 L2. Shown is the previously described region of DNA binding at the N terminus at residues 1 to 30, the two L1 interacting domains for capsid formation at residues 129 to

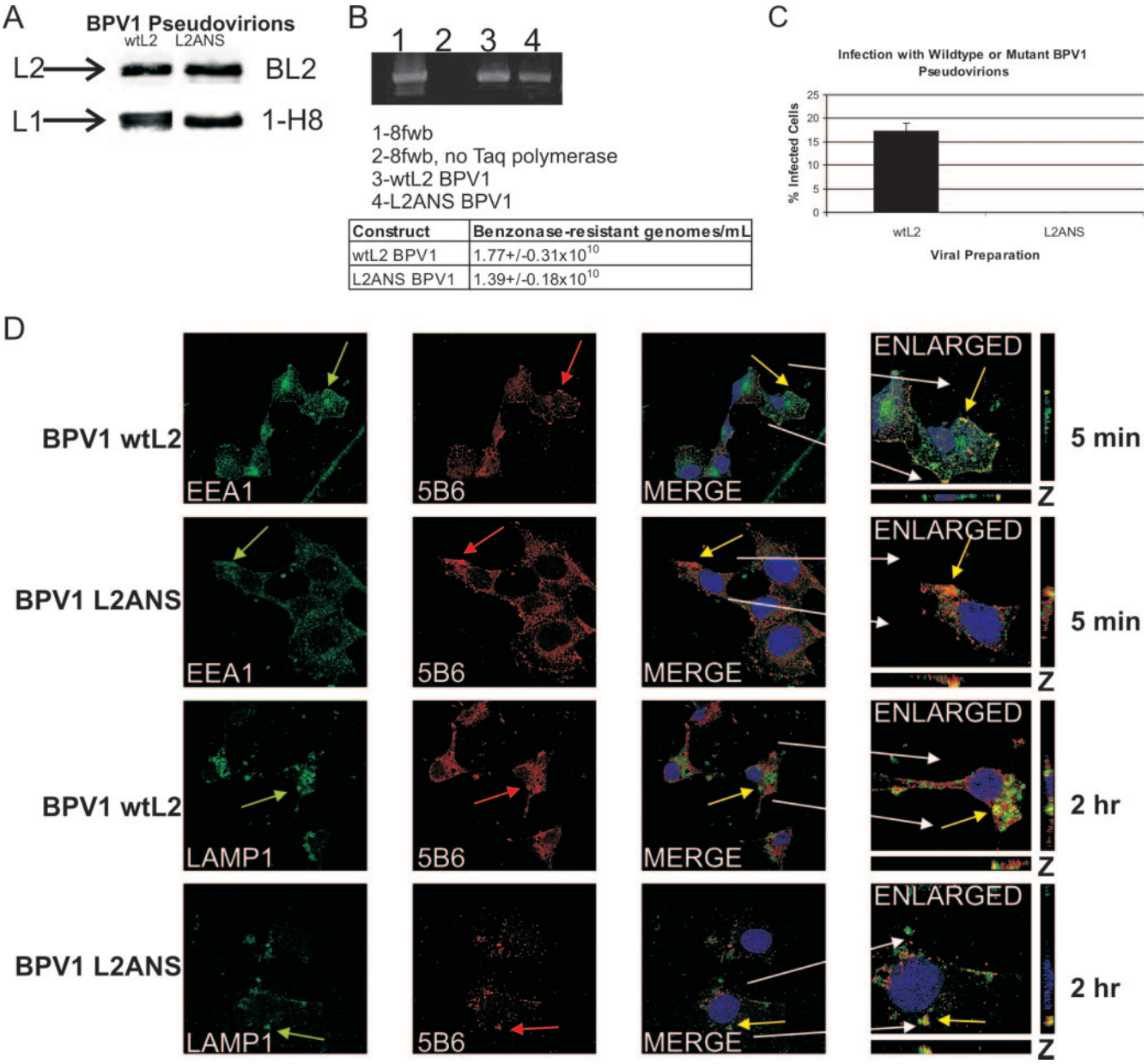

Construct	Benzonase-resistant genomes/mL
wtL2 BPV1	$1.77+/-0.31x10^{10}$
L2ANS BPV1	$1.39+/-0.18x10^{10}$

FIG. 1. Analysis of viral production and early trafficking of pseudovirions generated with L2 mutated at residues 41 to 44. (A) Protein lysates of benzonase-treated and overnight-matured BPV1 pseudovirions generated with wtL2 or the L2ANS mutant (L2ANS) protein were blotted for L2 (top) using BL2 and L1 (bottom) using 1-H8. (B) DNA extracted from L2 and L2ANS pseudovirions was PCR amplified for GFP cDNA sequences found in the packaged 8fwb plasmid. The PCR DNA gel was stained using SYBR green (top). Lane 1, 8fwb plasmid (positive control); lane2, 8fwb plasmid without *Taq* polymerase; lane 3, DNA extracted from BPV1 wtL2; lane 4, DNA from the BPV1 L2ANS pseudovirions. The table shows the number of encapsidated genomes obtained from real-time PCR analysis of the DNAs extracted from wtL2 and L2ANS pseudovirions. (C) FACS analysis (encapsidated 8fwb DNA encodes the GFP cDNA) was performed on COS-7 cells infected using equivalent numbers of genomes determined by real-time PCR of wtL2 BPV1 pseudovirions (black bar) (17.4%) or mutant L2ANS BPV1 pseudovirions (0% infection). The experiment shown was done in triplicate, and the error bar represents the standard deviation. (D) COS-7 cells infected with BPV1 wtL2 or L2ANS pseudovirions for 5 min were stained with antibody to EEA1 and the anti-L1 antibody 5B6 (top two rows, green arrows and red arrows, respectively). The wtL2 pseudovirions (top row) and the L2ANS pseudovirions (second row) show colocalization between 5B6 and EEA1 (yellow overlap in merged and enlarged panels). COS-7 cells infected with BPV1 wtL2 or L2ANS pseudovirions for 2 h were stained with the antibody to LAMP1 and the anti-L1 antibody 5B6 (bottom two rows, green arrows and red arrows, respectively). The wtL2 pseudovirions (third row) and the L2ANS pseudovirions (last row) show colocalization between 5B6 and LAMP1 (yellow overlap in merge and enlarged panels). The nuclei in the merge and enlarged images in all rows are stained with TOPRO-3 (blue). *z* sections are shown on the sides and bottoms of enlarged images.

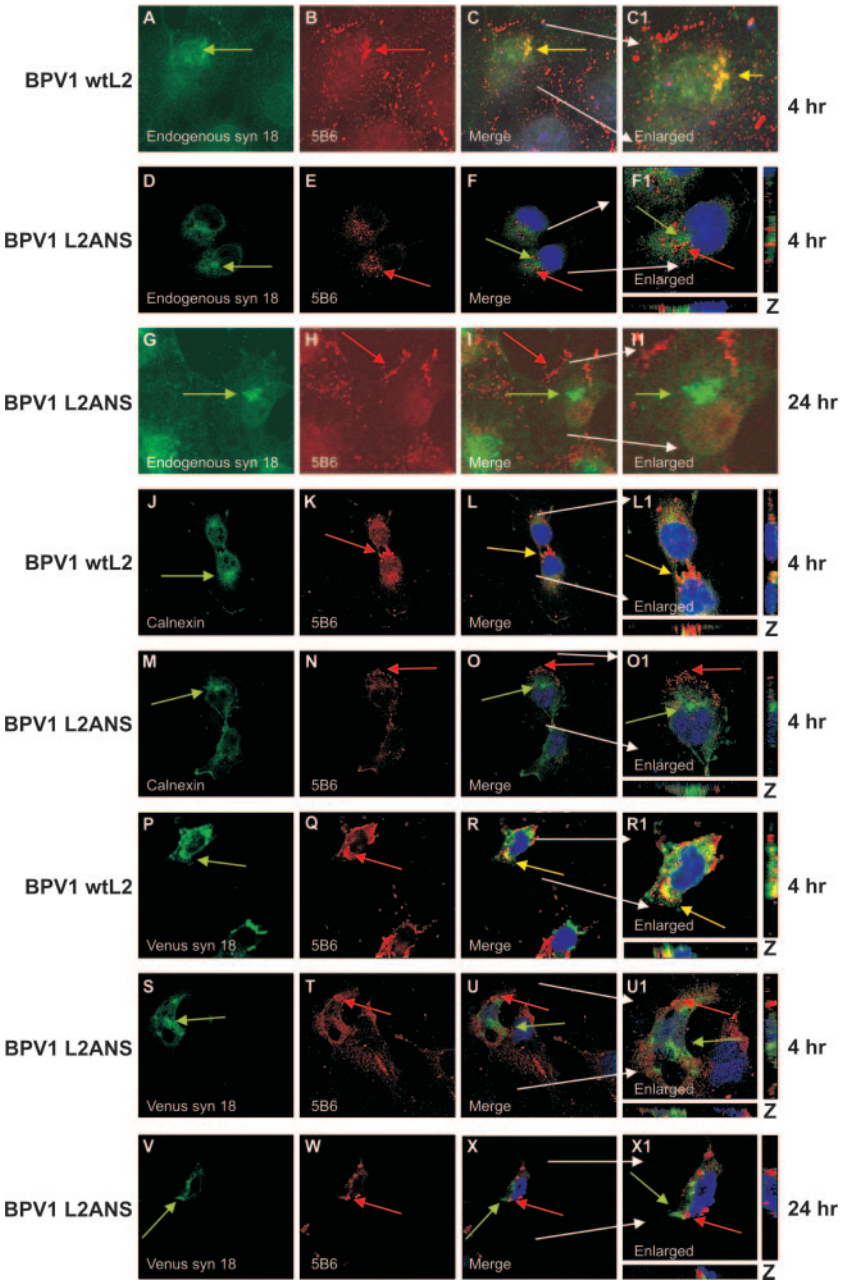

FIG. 2. The observed colocalization of BPV1 wtL2 pseudovirions and syntaxin 18 in COS-7 cells is lost when residues 41 to 44 of L2 are mutated. (A to C1) Cells infected with wtL2 BPV1 infectious pseudovirions for 4 h were stained with anti-syntaxin 18 (A, green arrow) and anti-L1 5B6 (B, red arrow) antibodies. At 4 h, the overlap of wild-type pseudovirions and endogenous syntaxin 18 is shown (C and C1, yellow overlap). (D to F1) Cells infected with BPV1 L2ANS noninfectious pseudovirions for 4 h were stained with anti-syntaxin 18 (D, green arrow) and 5B6 (E, red arrow). At 4 h, no overlap of endogenous syntaxin 18 and mutant pseudovirions was observed (F and F1). Even up to 24 h (G to I1), colocalization was not observed between endogenous syntaxin 18 (G, green arrow) and mutant BPV1 L2ANS pseudovirions stained with 5B6 (H, red arrow). Calnexin staining for the ER (J and M, green arrows) showed the overlap with wtL2 BPV1 (K, red arrow) at 4 h (L and L1, merged images, yellow arrows) but not with the L2ANS BPV1 (N, red arrow) at 4 h (O and O1, merged images). Cells transfected with venus (a GFP derivative)-tagged syntaxin 18 (P and S, green arrows) were infected for 4 h with wtL2 BPV1 pseudovirions (P to R1) or with L2ANS BPV1 pseudovirions (S to U1). wtL2 pseudovirions stained with 5B6 (P, red arrow) overlapped with venus syn 18 fluorescence (yellow arrows in merged images R and R1). There was no overlap of L2ANS pseudovirions stained with 5B6 (T, red arrow) and venus syn 18 (U and U1, merged images). Cells transfected with venus syn 18 were infected for 24 h with L2ANS pseudovirions (V to X1). There was no overlap of L2ANS pseudovirions stained with 5B6 (W) and venus syn 18 (X and X1, merged images). Nuclei (blue) were stained with DAPI (first and third rows) or TOPRO-3 (second and last five rows).

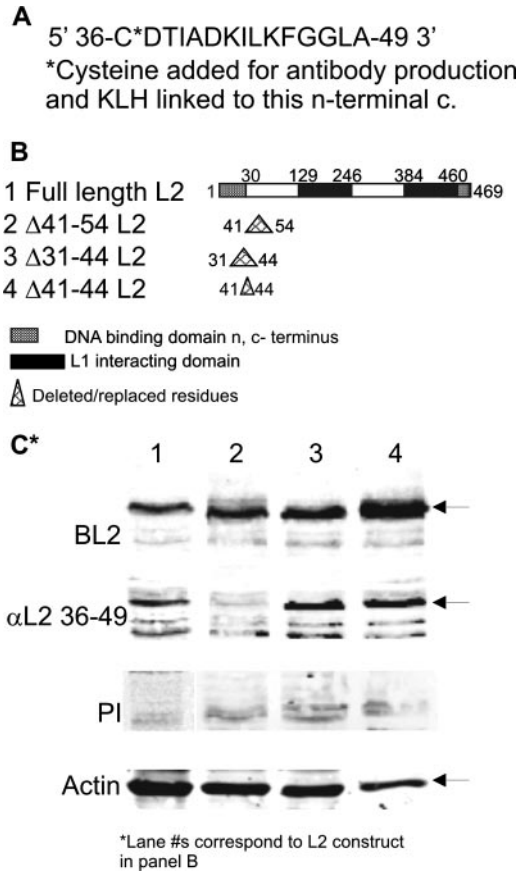

FIG. 3. Specificity of binding of αL2 36–49 antibody. (A) BPV1 L2 residues 36 to 49 with the addition of a C at the N terminus were linked to KLH for antibody production. (B) Lane 1, diagram of L2 indicating the DNA binding domains and the L1 interacting domains. A diagram of BPV1 L2 deleted of residues 41 to 54 (lane 2), 31 to 44 (lane 3), and 41 to 44 (lane 4) is shown. (C) Western blot of COS-7 cell lysates transfected with BPV1 full-length L2 (lane 1) or L2 deleted of residues 41 to 54 (lane 2), residues 31 to 44 (lane 3), or residues 41 to 44 (lane 4). Antibodies used were anti-full-length BPV1 L2 (top row), αL2 36–49 (second row), and preimmune serum (third row). Anti-actin, shown at the bottom, served as the loading control.

246 and 384 to 460, and the C-terminal DNA binding domain from residues 460 to 469 (14, 35). Also shown are the residues changed/deleted in the mutant constructs corresponding to amino acids 41 to 54, 31 to 44, or 41 to 44 (Fig. 3B, lanes 2 to 4, respectively). The constructs were made using standard PCR techniques to add an EcoRI (residues ANS) at the newly made junction as described previously (2). Lysates were run on a 10% resolving gel and blotted using the following four antibodies: (i) BPV1 antibody BL2 made against full-length BPV1 L2 (Fig. 3C, top panel); (ii) the antibody that we generated against residues 36 to 49, αL2 36–49 (Fig. 3C, second panel); (iii) the preimmune serum from the immunized rabbit (Fig. 3C, third panel); and (iv) anti-actin (Fig. 3C, bottom panel) to serve as the loading control. The various L2 constructs are expressed equally well compared to full-length L2 and are all recognized by the antibody generated against full-length L2 (Fig. 3C, top panel). αL2 36–49 detects the 62-kDa full-length capsid protein (Fig. 3C, second panel, lane 1) and detects both L2 mutants deleted of residues 31 to 44 and 41 to 44 (Fig. 3C, second panel, lanes 3 and 4, respectively). αL2 36–49 does not detect L2 with the deletion of amino acids 41 to 54 (Fig. 3C, second panel, lane 2). There is no detection of L2s using preimmune sera (Fig. 3C, third panel). The data for the analysis of the binding of αL2 36–49 show that we have an antibody that is specific for L2 at residues 36 to 49 and is dependent primarily on residues 45 to 49.

Antibody to L2 residues 36 to 49 binds to the outer surface of BPV1 pseudovirions. We used immunogold EM to analyze if affinity-purified αL2 36–49 could bind to pseudovirions. Double-Optiprep-purified BPV1 pseudovirions bound to carbon-filmed nickel grids were extensively blocked (see Materials and Methods) and incubated overnight at 4°C with anti-L1 5B6 and affinity-purified αL2 36–49 antibody (Fig. 4A) or 5B6 and affinity-purified rabbit anti-GST antibody as an isotypic control (Fig. 4B). Immunogold (10-nm)-labeled anti-mouse secondary antibody was used to detect 5B6, and immunogold (6-nm)-labeled anti-rabbit was used to detect αL2 36–49 or anti-GST antibodies. Grids were negatively stained to allow the visualization of the BPV1 pseudovirions at the expected diameter of 50 nm, and the gold particles were visible due to their higher density and are represented by black dots (Fig. 4). Analysis of the grids at a magnification of ×120,000 demonstrated the double labeling of particles with 5B6 (Fig. 4A, black double arrowhead) and affinity-purified αL2 36–49 (Fig. 4A, open arrowhead). When the pseudovirions were incubated with 5B6 and anti-GST, only 10-nm gold particles were observed (Fig. 4B, black double arrowhead), showing the binding of 5B6 but not of the isotypic affinity-purified control GST antibody. These results demonstrate that L2 residues 36 to 49 are exposed on viral particles that are properly formed as evident by the costaining with 5B6, and the EM images confirm that our viral preparation contains L1/L2 viral particles. We did not find any evidence that we had L1 pentamers in our double-purified pseudovirion preparations recognized by 5B6.

BPV1 infection is neutralized by antisera to BPV1 L2 residues 36 to 49. Since it was observed that the affinity-purified antibody against L2 residues 36 to 49 was binding to benzonase-treated, overnight-matured, and double-Optiprep-purified pseudoviruses, we wanted to address the effect that this antibody might have in neutralizing the infection of BPV1 pseudovirions and genuine virions (Fig. 5). We first tested the ability of the antisera obtained from the immunized rabbit to neutralize infection (Fig. 5A, black bars) and compared this to that of its preimmune serum (Fig. 5A, white bars). BPV1 pseudovirions containing GFP as a transgene were incubated with the sera for 30 min at 37°C and then added to ~100,000 COS-7 cells. Our titer was based on GFP-positive cells (obtained by FACS analysis), and experiments were performed with sufficient virus to infect approximately 5,000 cells. Infections were analyzed by FACS after 24 h. We observed a dose-dependent decrease in infection with the incubation of immune antisera compared to the preimmune sera: 13.3%, 30.5%, and 58.4% at 1/150, 1/60, and 1/30, respectively, (Fig. 5A). Our data demonstrate that an immune response to a single injection of residues 36 to 49 is capable of generating a modest level of neutralizing antibody.

We then wanted to address if this neutralization was indeed antibody specific and if it could be reproduced in C127 cells, a

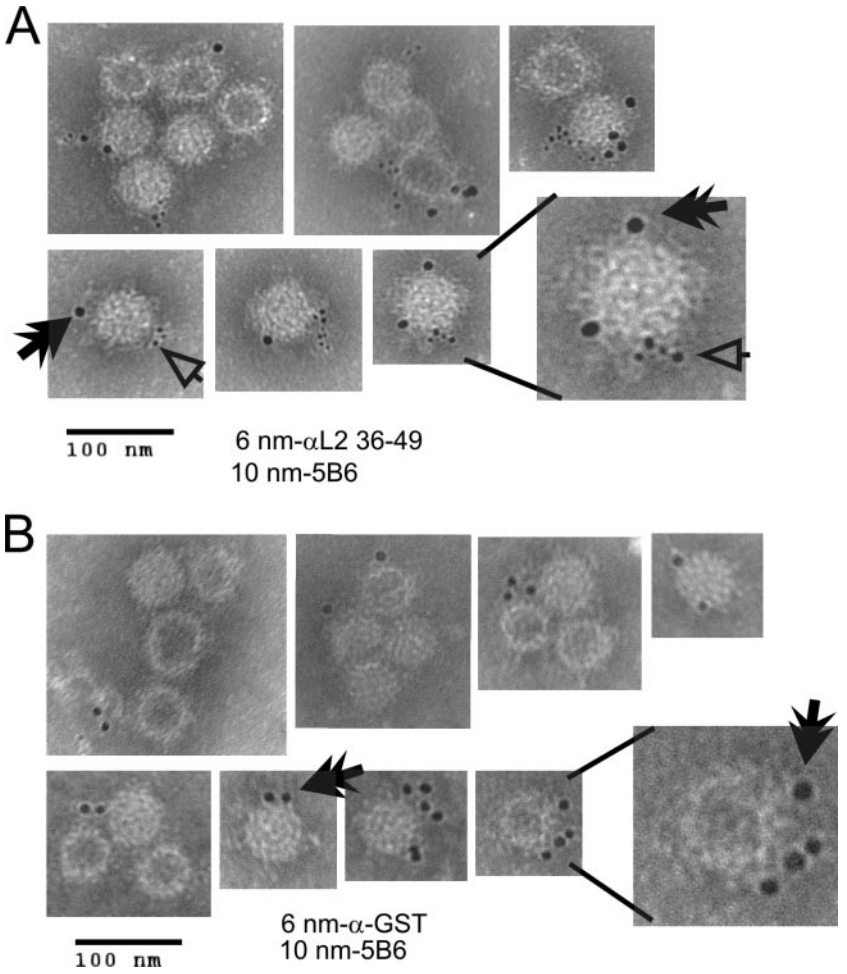

FIG. 4. EM analysis of affinity-purified αL2 36–49 binding to BPV1 pseudovirions. Double-Optiprep-purified BPV1 pseudovirions generated in 293TT cells were bound to carbon-filmed grids and incubated with affinity-purified rabbit αL2 36–49 and mouse anti-L1 5B6 antibodies (A) or the isotypic control affinity-purified rabbit anti-GST and 5B6 antibodies (B). The smaller black dots represent the 6-nm gold particle-labeled anti-rabbit secondary antibody used to detect αL2 36–49 or anti-GST (open arrowhead), and the larger black dots are the 10-nm anti-mouse immunogold secondary antibody used to detect 5B6 (black double arrowhead). The virus is seen as approximately 50 nm in diameter. The scale bar represents 100 nm. Magnification, ×120,000.

nontumorigenic mouse mammary tumor cell line susceptible to BPV1 infections (Fig. 5B). The infections with pseudovirions were analyzed at 48 h by FACS analysis (i.e., GFP-positive cells). We used the isotypic affinity-purified rabbit anti-GST antibody that did not bind to purified pseudovirions in our EM analysis as a control. C127 cells infected with BPV1 pseudovirions with the addition of 20 μg of anti-GST antibody (Fig. 4C, white bar) did not result in any decrease in infection. In contrast, the addition of 2, 10, and 20 μg of affinity-purified αL2 36–49 resulted in a 73.9%, 95.2%, and 98.2% loss of infection, respectively, compared to virus alone (Fig. 4C, gray bar). Each bar represents the average of three experiments counted by FACS, and error bars demonstrate the standard deviations in the experiments. These data demonstrate that our αL2 36–49 antibody can partially and fully neutralize infection of BPV1 pseudovirions in a susceptible cell line in a dose-dependent manner.

Since the integrity of the pseudovirions may be of concern (see Discussion), we addressed whether infection of genuine BPV1 virions obtained from warts could be affected by αL2 36–49. To determine if affinity-purified αL2 36–49 antibody could effectively reduce infection of genuine BPV1 virions, a focus-forming assay was performed on C127 cells (Fig. 5D). The genuine virions were Optiprep purified from a wart extract obtained from the ATCC and incubated with 50 or 100 μg of affinity-purified αL2 36–49 or with 100 μg of anti-GST control antibody for 1 h on ice before addition to cells. After 2 weeks, virally transformed C127 cells formed foci that were stained and counted. The addition of 50 μg and 100 μg of αL2 36–49 decreased the number of foci by 34% and 73%, respectively (50 μg, 32 foci; 100 μg, 13 foci) (Fig. 5D), compared to cells infected with virus alone (48 foci) (Fig. 5D, gray bar). Cells preincubated with 100 μg of anti-GST had 38 foci (Fig. 5D, white bar). Error bars demonstrate the standard deviations of three experiments. Similar dose-dependent and statistically significant results were observed in multiple experiments, and infection could be blocked by more than 73% by changing the virus-to-antibody ratio to favor the antibody and vice versa to

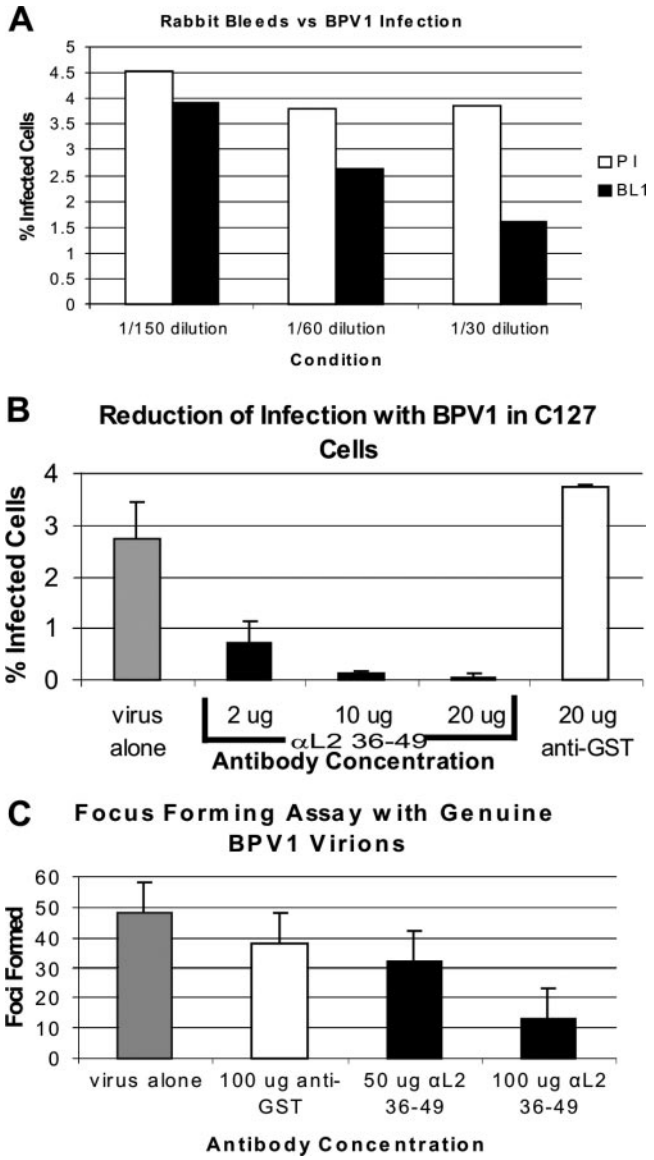

FIG. 5. Dose-dependent neutralization of BPV1 infections with affinity-purified αL2 36–49 antibody. (A and B) Pseudovirus-encapsidated 8fwb DNA encodes GFP cDNA. (A) FACS analysis of the percentage of COS-7 cells infected with pseudovirus preincubated with preimmune serum (PI) (white bars) compared to cells infected with pseudovirus preincubated with αL2 36-49-immunized sera (BL1) (black bars). Sera were used at 1/150, 1/60, and 1/30 dilutions. (B) FACS analysis of the percentage of C127 cells infected with BPV1 pseudovirions (gray bar); BPV1 pseudovirions and 2, 10, and 20 μg of affinity-purified αL2 36–49 (black bars); or 20 μg of the affinity-purified isotypic anti-GST antibody control antibody (white bar). Each bar represents an average of three infections, and error bars show the standard deviations. (C) A focus-forming assay was performed using C127 cells and genuine BPV1 virions. Two weeks after infection, the cell cultures were fixed and stained, and foci were counted. The numbers of foci from genuine virus-infected cells without the addition of antibody (gray bar), infection with the addition 100 μg of the isotypic control anti-GST (white bar), and 50 and 100 μg of αL2 36–49 (black bars) are shown. Error bars show the standard deviations from three experiments.

favor the number of foci. The block of the ability of genuine BPV1 to infect C127 cells supports the hypothesis that residues 36 to 49 are important in the infectious process and validates αL2 36–49 as a viable neutralizing antibody.

Neutralization of infection with affinity-purified αL2 36–49 is inhibited by a peptide of residues 36 to 49. In order to further demonstrate the specificity of inhibition of infection by the affinity-purified αL2 36–49 peptide, we performed a competition experiment with the peptide corresponding to BPV1 L2 residues 36 to 49 (wild-type peptide) and a control peptide of the same 15 residues in scrambled order. If neutralization was indeed targeted to residues 36 to 49, then incubation with the wild-type peptide sequence should block neutralization, and no block should be observed using the scrambled version of this sequence. Increasing concentrations of peptide were mixed with 20 μg of affinity-purified antibody prior to infection with BPV1 pseudovirions carrying the GFP transgene (Fig. 6A and B). For these experiments, we increased the infectious titer used to 20,000 infectious units in order to ensure that a linear dose-dependent effect on the block of infection was observed. Partial neutralization (~50%) of infection was observed with the addition of 20 μg of the affinity-purified αL2 36–49 antibody compared to virus alone (Fig. 6A and B, compare white bars with gray bars). The addition of the wild-type peptide corresponding to BPV1 L2 residues 36 to 49 resulted in a 6.9% loss of neutralization at 10 nM, a 45% loss at 100 nM, and a complete loss of the neutralizing activity of αL2 36–49 at 1 μM (Fig. 6A, 10 nM, 100 nM, and 1 μM bars). This dose-dependent loss in the inhibition of infection with the wild-type peptide was not observed when the affinity-purified αL2 36–49 antibody was incubated with the scrambled peptide at concentrations ranging from 10 nM to 1 μM (Fig. 6B, 10 nM, 100 nM, and 1 μM bars), nor was it observed at 10 and 100 μM (data not shown). These data confirm that the antibody was made against residues 36 to 49 and that the binding was dependent on a specific sequence order of the amino acids and not just amino acid content, i.e., charge or other peptide characteristic.

We then confirmed the results of the peptide competition assay in a focus-forming assay to determine the specificity of αL2 36–49 against genuine BPV1 virions. Optiprep-purified genuine infectious units added to C127 cells were increased in order to obtain an average of 122.7 foci with no antibody (Fig. 6C, first gray bar). When 200 μg of affinity-purified αL2 36–49 antibody was preincubated with the genuine virions, the number of foci was effectively reduced to 34, a 72% decrease (Fig. 6C, second white bar). This neutralization was not competed with the scrambled peptide (32 foci) (Fig. 6C, bar 3). In contrast, the addition of 10 μM wild-type sequence L2 peptide at residues 36 to 49 resulted in 116 foci, comparable to infection with virus alone and thus a complete block or competition of neutralization (Fig. 6C, bar 4). The numbers of foci from three separate 60-mm^2 dishes from a single experiment were averaged, and standard deviations are represented by the error bars. These data show that the neutralization of genuine BPV1 was also specifically blocked with αL2 36–49, i.e., targeted to L2 residues 36 to 49.

Addition of affinity-purified antibody after pseudovirions have bound to the cell surface enhances neutralization. In the above-described neutralization experiments with affinity-purified αL2 36–49, unbound virus and antibody were not removed

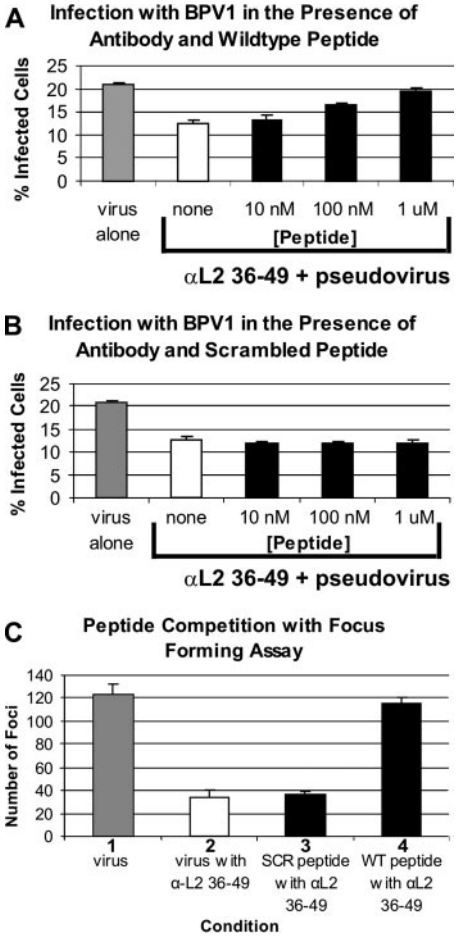

FIG. 6. Neutralization of BPV1 infection by αL2 36–49 antibody can be competed with a peptide corresponding to residues 36 to 49. (A and B) Pseudovirus-encapsidated DNA of 8fwb encodes the GFP cDNA, and infections were analyzed by FACS. C127 cells were infected with pseudovirions alone (gray bar) (same data in A and B) in the presence of affinity-purified αL2 36–49 antibody (white bar) (same data in A and B) or (A) antibody that was preincubated with BPV1 L2 peptide at residues 36 to 49 in increasing concentrations of 10 nM, 100 nM, and 1 μM (black bars). An increase in infection signifies a loss of neutralization in the presence of the added peptide. (B) Antibody was preincubated with scrambled BPV1 L2 peptide at residues 36 to 49 in increasing concentrations of 10 nM, 100 nM, and 1 μM (black bars). No increase in infection was observed; thus, scrambled peptide does not interfere with the neutralization by αL2 36–49. Data bars represent the averages of three experiments, and standard deviations are demonstrated by error bars. (C) Focus-forming assay of C127 cells infected with genuine BPV1 virions. Bar 1, number of foci formed from the addition of virions alone; bar 2, foci formed with the addition of αL2 36–49; bar 3, foci formed with antibody and scrambled BPV1 L2 peptide at residues 36 to 49 (no loss of neutralization was observed); bar 4, foci formed with antibody and 10 μM wild-type BPV1 L2 peptide at residues 36 to 49. A complete loss of neutralization was observed. C127 cell foci were visible after staining with methylene blue. Data represent average numbers of foci formed in three plates under the same conditions. Standard deviations are shown by error bars.

prior to allowing the infection to proceed. This prevented us from determining whether the observed neutralization was due to the initial binding of the antibody to the viral capsid or if there was a conformational change in the viral capsid after it had bound to the cellular receptor, making the epitope more

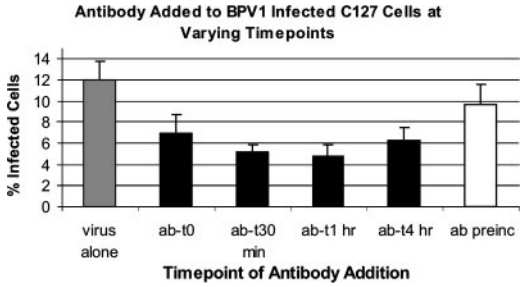

FIG. 7. The ability of αL2 36–49 to neutralize infection is increased after virus has bound to the target cells. C127 cells were infected with BPV1 pseudovirions containing the 8fwb GFP plasmid and analyzed by FACS. In all conditions, pseudovirions were incubated with cells for 2 h on ice, and unbound pseudovirions (and antibody in preincubation) were removed prior to returning cells to 37°C and 5% CO_2. The gray bar represents the percentage of cells infected with pseudovirus alone; the white bar represents the percentage of cells incubated with pseudovirus that was preincubated with αL2 36–49 for 1 h. Data for the addition of αL2 36–49 to infected cultures immediately after the 2 h incubation on ice (ab-t0) and after 30 min (ab-t30 min), 1 h (ab-t1 h), and 4 h (ab-t4 h) postinfection, i.e., after cells were returned to 37°C and 5%CO_2, are shown. Data represent the means of three experiments; standard deviations are shown by the error bars.

accessible to the antibody (41, 46, 52). BPV1 pseudovirions carrying the GFP transgene were allowed to bind to the surface of C127 cells on ice for 2 h, unbound virus was removed by washing the cells with medium, and plates were placed at 37°C for virus internalization. Twenty micrograms of affinity-purified αL2 36–49 was added at various time points after viral entry had begun. As shown in Fig. 7 (gray bar), the addition of BPV1 pseudovirions without antibody resulted in the infection of 11.94% of cells. As described above, preincubating the virus with the antibody followed by washing of excess virus and antibody lowered the infection level to 9.75% (Fig. 7, white bar). In contrast, the addition of αL2 36–49 antibody immediately after the 2-h infection at 4°C, i.e., when cells were moved to 37°C, lowered infection to 7% of cells (Fig. 7, ab-t0 bar). The addition of αL2 36–49 antibody 30 min and 1 h postincubation lowered the infection levels to 5.2% and 4.8%, respectively, a 60% decrease in infection when added after 1 h compared to an 18% decrease in infection when the antibody was preincubated (Fig. 7). The addition of antibody after 4 h, which has been described as the half-life of entry for BPV1 (13), lowered the infection to 6.21%, a loss of neutralization from the addition of antibody after 1 h. These data support the finding that although binding to free virus by αL2 36–49 partially neutralizes infection, a more robust neutralization is observed after the pseudovirus binds to the cell membrane. This increase in neutralization may be due to a conformational change of the viral capsid after binding to the cells that increases the affinity of antibody binding or makes the epitope more accessible to the antibody. These data also support the finding that after 4 h, much of the bound PVs have internalized (13) due to a decrease in the ability of αL2 36–49 antibody to block infection.

αL2 36–49 interferes with the coimmunoprecipitation of BPV1 L2 and syntaxin 18 proteins and the colocalization of BPV1 pseudovirions with syntaxin 18 during infection. We previously showed that BPV1 L2 and FLAG-syntaxin 18 co-

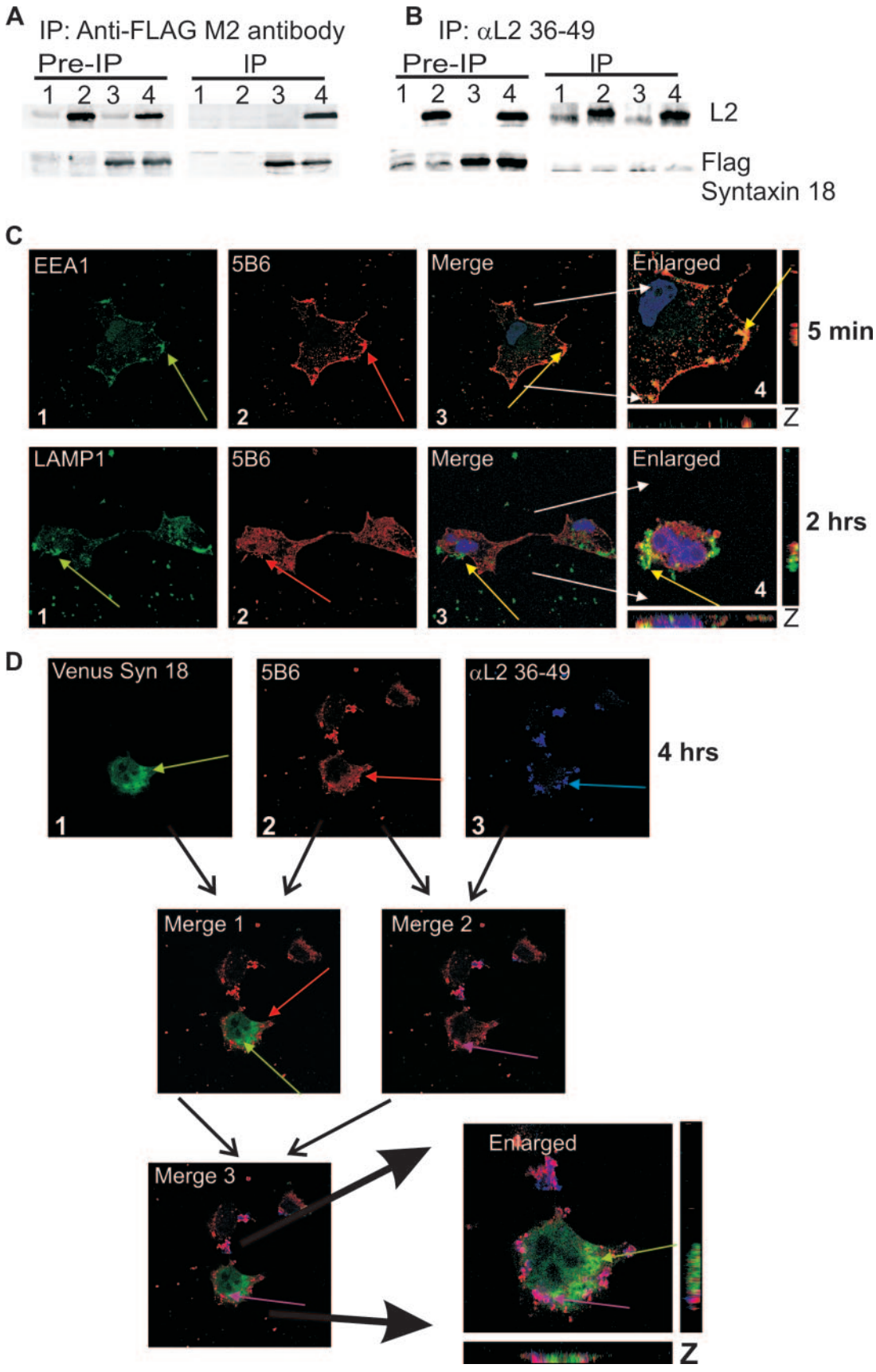
A
IP: Anti-FLAG M2 antibody
Pre-IP
IP
1 2 3 4 1 2 3 4
B
IP: αL2 36-49
Pre-IP
IP
1 2 3 4 1 2 3 4
L2
Flag
Syntaxin 18
C
EEA1
5B6
Merge
Enlarged
1
2
3
4
Z
5 min
LAMP1
5B6
Merge
Enlarged
1
2
3
4
Z
2 hrs
D
Venus Syn 18
5B6
αL2 36-49
1
2
3
4 hrs
Merge 1
Merge 2
Merge 3
Enlarged
Z

immunoprecipitated when cotransfected (2). Our coimmunoprecipitation pull-down experiments again demonstrate the following: (i) FLAG-syntaxin 18 can coimmunoprecipitate with untagged BPV1 L2 (Fig. 8A, lane 4), (ii) the M2-FLAG antibody bound to Sepharose beads does not precipitate L2 nonspecifically (Fig. 8A, lane 2), (iii) we did not precipitate a nonspecific band at the size of BPV1 L2 in vector control-transfected cells (Fig. 8A, lane 1), and (iv) M2-FLAG-coated beads do immunoprecipitate the FLAG-syntaxin 18 protein (Fig. 8A, lanes 3 and 4). To determine if αL2 36–49 was interfering with the ability of L2 to interact with syntaxin 18, we attempted to coimmunoprecipitate BPV1 L2 and FLAG-syntaxin 18 with αL2 36–49 antibody. BPV1 L2 was immunoprecipitated specifically with αL2 36–49 antibody (Fig. 8B, lanes 2 and 4), and FLAG syntaxin 18 did not nonspecifically bind to the protein A/G beads and αL2 36–49 (Fig. 8B, lane 3). We did not coimmunoprecipitate FLAG-syntaxin 18 with BPV1 L2 (Fig. 8B, lane 4). Preimmunoprecipitation blots show 2.5% of input lysates, and vector control-transfected cell are shown in Fig. 8 (lanes 1). Antibodies to full-length BPV1 L2 and anti-FLAG-M2 antibody were used to detect the proteins in Western blots. The Western blot shows that the L2 αL2 36–49 antibody interferes with the interaction of syntaxin 18 protein with BPV1 L2 protein. In vitro cell-free work is in progress to determine if the interaction of the L2 protein with syntaxin 18 is direct or indirect.

Since we observed that αL2 36–49 interfered with the coimmunoprecipitation of the L2 protein with syntaxin 18, we wanted to determine if neutralization was a result of αL2 36–49 preventing the interaction of pseudovirions with syntaxin 18 (as shown in Fig. 2). We first addressed if the addition of this neutralization antibody was interfering with the early entry of the pseudovirions. Our data determined that the addition of αL2 36–49 did not interfere with the movement of BPV1 wtL2 pseudovirions into an EEA1- or a LAMP1-positive vesicle (Fig. 8C). Staining for pseudovirions that were preincubated for 1 h on ice with αL2 36–49 demonstrated overlap with EEA1 at 5 min (Fig. 8C, top row, merge) and LAMP1 at 2 h (Fig. 8C, bottom row, merge). Under these conditions, cultures had a >95% loss of infection at 48 h (data not shown). These data show that αL2 36–49 was not blocking the initial endocytosis of the virions, and, as with our L2ANS pseudovirion, the data show that residues 36 to 49 are not involved in the initial entry of the pseudovirions.

To address whether the addition of αL2 36–49 resulted in the lack of interaction between BPV1 pseudovirions and syntaxin 18 during infection, we performed confocal immunofluorescence analysis of the infection of COS-7 cells transfected with 500 ng of venus syn 18 in the presence of αL2 36–49. VENUS syn 18-transfected cells were incubated with BPV1 pseudovirions that were preincubated with αL2 36–49. After 4 h of infection, cells were fixed and stained for 5B6 and secondary donkey anti-rabbit antibodies (Alexa Fluor 647) to detect the presence of αL2 36–49. Samples were viewed by confocal microscopy using 488-, 597-, and 642-nm exciting lasers in order to see all three colors. Syntaxin 18 (Fig. 8D1, green arrow) and 5B6 (Fig. 8D2, red arrow) did not show overlap at 4 h (Fig. 8D, merge 1). Overlap was observed between 5B6 and αL2 36–49 (Fig. 8D3, blue arrow), shown by the image in which VENUS syn 18 fluorescence has been omitted (Fig. 8D, merge 2, violet arrow). The overlay of venus syn 18, 5B6, and αL2 36–49 fluorescence suggests that there is no colocalization of the virus with syntaxin 18 in the presence of αL2 36–49 (Fig. 8D, merge 3 and enlarged image). The data in this experiment showing that the loss of the interaction of the 5B6-stained pseudovirion with syntaxin 18 in the presence of αL2 36-49-bound pseudovirions correlate with a loss of infection, confirming that the infection of BPV1 is in part dependent on syntaxin 18 and mediated by L2 residues 36 to 49.

DISCUSSION

The PV L2 minor capsid protein has been demonstrated to be involved in facilitating infection and to contribute to DNA packaging (28, 52). Our laboratory previously identified the interaction of the BPV1 L2 protein with the intracellular trafficking protein syntaxin 18 (2). Syntaxin 18 was originally identified as having a role in vesicle trafficking between the ER, the intermediate compartment, and the *cis*-Golgi compartment (26) and has recently been purified from phagosomes containing endocytic markers including EEA1 (27). We had shown that the loss of an L2 protein interaction with syntaxin 18 was achieved by replacing residues 41-DKILK-44 of BPV1 L2 with 41-ANS-44 (L2ANS, where ANS is an EcoRI site). This suggested that L2 residues 41 to 44 were directly or indirectly mediating the interaction with syntaxin 18 or were responsible for the trafficking of L2 to a cellular region where this interaction occurred. In addition, although the DNA packaging efficiency, L1-to-L2 capsid ratio, and morphology by EM of pseudovirions generated with L2ANS were similar to those of pseudovirions generated with wtL2, L2 ANS BPV1 pseudovirions were noninfectious.

FIG. 8. αL2 36–49 antibody interferes with the interactions of syntaxin 18 with L2 protein and wtL2 pseudovirions. (A and B) Cells were transfected with control vector pA3M (lane 1), pA3M and BPV1 L2 (lane 2), pA3M and FLAG-syntaxin 18 (lane 3), or BPV1 L2 and FLAG-syntaxin 18 (lane 4). Samples were immunoprecipitated (IP) with FLAG M2 antibody-coated beads (A) or αL2 36–49 (B). Western blots for L2 (top) and FLAG-syntaxin 18 (bottom) are shown. (C) αL2 36–49 antibody does not interfere with early viral entry. COS-7 cells were infected with wtL2 BPV1 pseudovirions preincubated with αL2 36–49 antibody for 5 min (top row) or 2 h (bottom row). Cells infected for 5 min (top row) were stained with anti-EEA1 (first panel, green arrow) and 5B6 (second panel, red arrow); cells infected for 2 h (bottom row) were stained with anti-LAMP1 (panel 1, green arrow) and 5B6 (panel 2, red arrow). Colocalization of the wtL2 pseudovirions and EEA1 or LAMP1 was not impeded by the presence of αL2 36–49 (top and bottom rows, panels 3 and 4, yellow arrows in the merged and enlarged images). (D) The addition of αL2 36–49 prevents the colocalization of BPV1 pseudovirions with syntaxin 18 at 4 h. Shown are VENUS syn 18 fluorescence (D1) (green arrow), BPV1 pseudovirions stained with 5B6 (D2) (red arrow), and staining of the αL2 36–49 pseudovirion-bound antibody (D3) (blue arrow). Merge 1 shows the overlay and lack of signal overlap of VENUS syn 18 and 5B6; merge 2 shows the overlap of signals for 5B6 and αL2 36–49, which results in a violet color (violet arrow); merge 3 and the enlarged image show the overlay of VENUS syn18, 5B6, and αL2 36–49 staining. The overlap of 5B6 and αL2 36–49 antibody staining (violet arrow) does not overlap with VENUS syn 18 (green arrow).

In this study, we analyzed the process of viral entry/infection by defining the relationship of pseudovirions and syntaxin 18. We were able to observe the overlap fluorescence of infectious BPV1 pseudovirions made with wtL2 with syntaxin 18 at 4 h as well as the ER marker calnexin. In contrast, overlap of syntaxin 18 (and calnexin) staining and staining of the noninfectious L2ANS BPV1 pseudovirions were not observed at any time point (Fig. 2). These data suggested that syntaxin 18 was playing a role during infection and that L2 residues 41 to 44 were contributing to the movement of viral particles into syntaxin 18-positive vesicles. We tested the possibility that the L2ANS pseudovirions were unable to use the entry mechanism used by wtL2 pseudovirions, specifically, the endocytic mechanism mediated by clathrin and involving the endocytic and lysosome marker EEA1 or LAMP1 as described previously (13) (Fig. 1 and 2). To our surprise, L2ANS and wtL2 were indistinguishable in their initial entries; i.e., L2ANS noninfectious pseudovirions interacted with both EEA1 and LAMP1, demonstrating that L2 residues 41 to 44 were not responsible for the initial entry of the pseudovirions into the target cells. We concluded that L2 residues 41 to 44 do not mediate the initial entry of the pseudovirions but rather mediate a later process involving syntaxin 18 that is necessary for infection.

Although L2 antibodies have been previously shown to neutralize infection, (8, 22, 29, 32, 42), the exact mechanism of this block has not been defined. Roden et al. and Gaukroger et al. (22, 42) previously identified that the N terminus of L2 was a sufficient target for neutralization that did not prevent binding or entry into cells. No mechanism of neutralization was shown in the previous works mentioned above, and thus, we cannot comment if their observed neutralization is occurring by the same mechanism as what we found. Our data are consistent with the finding that targeting the N terminus is neutralizing at a stage after binding and entry. The role of L2 during early entry has been shown to be primarily after virus binding and has been attributed to the findings that parts of the N terminus of L2 seem to loop out of the viral capsid in the fully formed particle or are exposed after a conformational change that occurs after the virus binds to the target cells (29, 30, 32, 36, 41, 43, 46, 48, 52). It was previously suggested that the L2 region encompassing residues 41 to 44 was exposed on the outside of pseudoviral particles using an enzyme-linked immunosorbent trap assay (30), but this has not been confirmed by EM. In this study, we demonstrate by EM that an antibody against L2 residues 36 to 49 (αL2 36–49) can bind to free BPV1 pseudovirion particles that have undergone an overnight maturation step. Our Western blotting analysis suggests that the αL2 36–49 antibody may require primarily L2 residues 45 to 49, since we observed binding to L2 mutants deleted of residues 31 to 44 and not of residues 41 to 54, leaving residues 45 to 49 as the necessary residues. Although it has been suggested that immature particles are fragile and may not survive the purification process (6), we cannot ignore the possibility that some of the double-purified viral particles in our EM analysis that are bound by αL2 36–49 have not fully matured. Regardless, even if these fragile particles may not be mature, they have been shown to retain their infectious capability (6), and as we show in Fig. 4, binding to residues 36 to 49 occurs simultaneously with the binding of 5B6, a neutralizing anti-L1 antibody that is dependent on the proper formation of viral particles. We are attempting to purify sufficient genuine BPV1 virions from warts to confirm our EM data.

Although we show that the affinity-purified antibody αL2 36–49 can bind to free viral particles and may thus neutralize infection (Fig. 4, 5, and 6), our data support previously described observations by others that there is a conformational change after the virus binds to the target cells that exposes the L2 N terminus (41, 46, 52). In our studies, neutralization was increased when αL2 36–49 was added after pseudovirions had bound to the target cells (Fig. 7). These neutralization data suggest that (i) the antibody can be bound to the viral particles with higher affinity after the virus has bound to the target cells, (ii) a conformational change occurs upon binding to the cell membrane that further exposes L2 residues 36 to 49, and/or (iii) incubation of pseudovirions at 37°C after Optiprep purification (for 30 min or 1 h) confers further maturation and changes in the regions of L2 that are exposed. We are addressing these three scenarios. The maturation status of genuine BPV1 virions obtained from warts from the ATCC is not known. However, the ability to neutralize these genuine BPV1 preparations that are capable of transforming cells, as evident by the decreasing number of foci in our focus-forming-unit assay, suggests that residues 36 to 49 are a real-life target for neutralization regardless of any virion maturity or virion conformational changes at the cell surface.

We hypothesize that syntaxin 18 is required for PV infection and that L2 mediates this interaction. Our analyses of the initial events in PV internalization showing the overlap of pseudovirions with EEA1 and LAMP1 recapitulate previously described studies (13, 41). Those studies could not distinguish between the staining of infectious and noninfectious viral particles. In our experiments, we show that infectious and noninfectious pseudoviral particles (wt L2 versus L2ANS pseudovirions) can overlap with EEA1- and LAMP1-positive vesicles, but we indeed show that only the infectious pseudoviral particles overlap with syntaxin (Fig. 2 and 8). To our knowledge, this is the first clear demonstration using a cellular marker for a cellular compartment of a difference in trafficking/localization between infectious and noninfectious PV virions or pseudovirions. Furthermore, to our knowledge, the loss of the colocalization of infectious pseudovirions with syntaxin 18 is the first data describing a mechanism of how a neutralizing antibody to L2 prevents infection intracellularly.

PV pseudoviruses have been shown to undergo an L2 furin cleavage event in the endosome during infection that allows for endosomal escape (41). Our data suggest that after endosomal escape, the next possible step is the association of the cleaved viral particle with a syntaxin 18-positive vesicle for trafficking towards the nucleus. More work needs to be done to determine if only L2 remains intact after endosomal escape and whether it is L2's trafficking to the nucleus with the bound encapsidated genome that is being mediated by syntaxin 18 rather than a modified partially denatured virion as occurs with adenovirus (reviewed in reference 33). Our staining of noninfectious virions with L1 antibody 5B6 at 24 h (Fig. 2) suggests that the L2ANS noninfectious pseudovirions have not undergone the disassembly event that results in the loss of 5B6 staining of the infectious pseudovirions at around 5 to 6 h. In addition, we were able to costain for L1 with 5B6 and bound αL2 36–49 with rabbit secondary antibody after 24 h, suggesting that the anti-

body was perhaps also preventing the disassembly of the wtL2 pseudovirion (data not shown). By use of EM of infected cells, we are addressing whether a loss of disassembly results in the loss of infection or if the observed staining pattern is of disassembled L1 and L2 components in an inappropriate vesicle, suggesting an error in trafficking. It is interesting that the amino acid sequence of L2 described as being important for the interaction with syntaxin 18, mainly DKILK, is identical to sequences found in capsid/envelope proteins of numerous viruses including picornavirus, human immunodeficiency virus, and blue tongue virus and is highly conserved in all PV genotypes.

ACKNOWLEDGMENTS

This work was supported by the H. M. Bligh Cancer Research Laboratory of the Rosalind Franklin University of Medicine and Science, North Chicago, IL, and by NIH/NCI grant K22:CA117971 to P.I.M.

P.I.M. thanks J. Dalmau and M. Rosenfeld for their support. We thank Figen Seiler for her support with electron microscopy (Rosalind Franklin University of Medicine and Science) and Daniel DiMaio at Yale University for his advice on setting up the focus-forming assays. We thank B. Chandran (Rosalind Franklin University of Medicine and Science) for helpful suggestions in preparing the manuscript.

REFERENCES

1. **Bordeaux, J., S. Forte, E. Harding, M. S. Darshan, K. Klucevsek, and J. Moroianu.** 2006. The L2 minor capsid protein of low-risk human papillomavirus type 11 interacts with host nuclear import receptors and viral DNA. J. Virol. **80:**8259–8262.
2. **Bossis, I., R. B. Roden, R. Gambhira, R. Yang, M. Tagaya, P. M. Howley, and P. I. Meneses.** 2005. Interaction of tSNARE syntaxin 18 with the papillomavirus minor capsid protein mediates infection. J. Virol. **79:**6723–6731.
3. **Bousarghin, L., A. Touze, P. Y. Sizaret, and P. Coursaget.** 2003. Human papillomavirus types 16, 31, and 58 use different endocytosis pathways to enter cells. J. Virol. **77:**3846–3850.
4. **Buck, C. B., D. V. Pastrana, D. R. Lowy, and J. T. Schiller.** 2004. Efficient intracellular assembly of papillomaviral vectors. J. Virol. **78:**751–757.
5. **Buck, C. B., D. V. Pastrana, D. R. Lowy, and J. T. Schiller.** 2005. Generation of HPV pseudovirions using transfection and their use in neutralization assays. Methods Mol. Med. **119:**445–462.
6. **Buck, C. B., C. D. Thompson, Y. Y. Pang, D. R. Lowy, and J. T. Schiller.** 2005. Maturation of papillomavirus capsids. J. Virol. **79:**2839–2846.
7. **Campo, M. S.** 2002. Animal models of papillomavirus pathogenesis. Virus Res. **89:**249–261.
8. **Christensen, N. D., and J. W. Kreider.** 1991. Neutralization of CRPV infectivity by monoclonal antibodies that identify conformational epitopes on intact virions. Virus Res. **21:**169–179.
9. **Crum, C. P., M. Symbula, and B. E. Ward.** 1989. Topography of early HPV 16 transcription in high-grade genital precancers. Am. J. Pathol. **134:**1183–1188.
10. **Culp, T. D., N. M. Cladel, K. Balogh, L. R. Budgeon, A. Mejia, and N. D. Christensen.** 2006. Papillomavirus particles assembled in 293TT cells are infectious in vivo. J. Virol. **80:**11381–11384.
11. **Darshan, M. S., J. Lucchi, E. Harding, and J. Moroianu.** 2004. The L2 minor capsid protein of human papillomavirus type 16 interacts with a network of nuclear import receptors. J. Virol. **78:**12179–12188.
12. **Day, P. M., C. C. Baker, D. R. Lowy, and J. T. Schiller.** 2004. Establishment of papillomavirus infection is enhanced by promyelocytic leukemia protein (PML) expression. Proc. Natl. Acad. Sci. USA **101:**14252–14257.
13. **Day, P. M., D. R. Lowy, and J. T. Schiller.** 2003. Papillomaviruses infect cells via a clathrin-dependent pathway. Virology **307:**1–11.
14. **Day, P. M., R. B. Roden, D. R. Lowy, and J. T. Schiller.** 1998. The papillomavirus minor capsid protein, L2, induces localization of the major capsid protein, L1, and the viral transcription/replication protein, E2, to PML oncogenic domains. J. Virol. **72:**142–150.
15. **Deau, M. C., M. Favre, and G. Orth.** 1991. Genetic heterogeneity among human papillomaviruses (HPV) associated with epidermodysplasia verruciformis: evidence for multiple allelic forms of HPV5 and HPV8 E6 genes. Virology **184:**492–503.
16. **DiMaio, D.** 1986. Nonsense mutation in open reading frame E2 of bovine papillomavirus DNA. J. Virol. **57:**475–480.
17. **Doorbar, J., and P. H. Gallimore.** 1987. Identification of proteins encoded by the L1 and L2 open reading frames of human papillomavirus 1a. J. Virol. **61:**2793–2799.
18. **Fay, A., W. H. Yutzy IV, R. B. Roden, and J. Moroianu.** 2004. The positively charged termini of L2 minor capsid protein required for bovine papillomavirus infection function separately in nuclear import and DNA binding. J. Virol. **78:**13447–13454.
19. **Fligge, C., F. Schafer, H. C. Selinka, C. Sapp, and M. Sapp.** 2001. DNA-induced structural changes in the papillomavirus capsid. J. Virol. **75:**7727–7731.
20. **Florin, L., K. A. Becker, C. Lambert, T. Nowak, C. Sapp, D. Strand, R. E. Streeck, and M. Sapp.** 2006. Identification of a dynein interacting domain in the papillomavirus minor capsid protein L2. J. Virol. **80:**6691–6696.
21. **Garcia-Pineres, A. J., A. Hildesheim, M. Trivett, M. Williams, L. Wu, V. N. Kewalramani, and L. A. Pinto.** 2006. Role of DC-SIGN in the activation of dendritic cells by HPV-16 L1 virus-like particle vaccine. Eur. J. Immunol. **36:**437–445.
22. **Gaukroger, J. M., L. M. Chandrachud, B. W. O'Neil, G. J. Grindlay, G. Knowles, and M. S. Campo.** 1996. Vaccination of cattle with bovine papillomavirus type 4 L2 elicits the production of virus-neutralizing antibodies. J. Gen. Virol. **77:**1577–1583.
23. **Ghys, P. D., C. Jenkins, and E. Pisani.** 2001. HIV surveillance among female sex workers. AIDS **15**(Suppl. 3)**:**S33–S40.
24. **Gissmann, L., H. Pfister, and H. Zur Hausen.** 1977. Human papilloma viruses (HPV): characterization of four different isolates. Virology **76:**569–580.
25. **Hanover, J. A., L. Beguinot, M. C. Willingham, and I. H. Pastan.** 1985. Transit of receptors for epidermal growth factor and transferrin through clathrin-coated pits. Analysis of the kinetics of receptor entry. J. Biol. Chem. **260:**15938–15945.
26. **Hatsuzawa, K., H. Hirose, K. Tani, A. Yamamoto, R. H. Scheller, and M. Tagaya.** 2000. Syntaxin 18, a SNAP receptor that functions in the endoplasmic reticulum, intermediate compartment, and cis-Golgi vesicle trafficking. J. Biol. Chem. **275:**13713–13720.
27. **Hatsuzawa, K., T. Tamura, H. Hashimoto, H. Hashimoto, S. Yokoya, M. Miura, H. Nagaya, and I. Wada.** 2006. Involvement of syntaxin 18, an endoplasmic reticulum (ER)-localized SNARE protein, in ER-mediated phagocytosis. Mol. Biol. Cell **17:**3964–3977.
28. **Holmgren, S. C., N. A. Patterson, M. A. Ozbun, and P. F. Lambert.** 2005. The minor capsid protein L2 contributes to two steps in the human papillomavirus type 31 life cycle. J. Virol. **79:**3938–3948.
29. **Kawana, K., H. Yoshikawa, Y. Taketani, K. Yoshiike, and T. Kanda.** 1999. Common neutralization epitope in minor capsid protein L2 of human papillomavirus types 16 and 6. J. Virol. **73:**6188–6190.
30. **Kondo, K., Y. Ishii, H. Ochi, T. Matsumoto, H. Yoshikawa, and T. Kanda.** 2007. Neutralization of HPV16, 18, 31, and 58 pseudovirions with antisera induced by immunizing rabbits with synthetic peptides representing segments of the HPV16 minor capsid protein L2 surface region. Virology **358:**266–272.
31. **Koutsky, L., T. Wright, and C. Ebel.** 2004. HPV in 2004: public health response to new tools. CDC National STD Prevention Conference. Centers for Disease Control and Prevention, Atlanta, GA.
32. **Liu, W. J., L. Gissmann, X. Y. Sun, A. Kanjanahaluethai, M. Muller, J. Doorbar, and J. Zhou.** 1997. Sequence close to the N-terminus of L2 protein is displayed on the surface of bovine papillomavirus type 1 virions. Virology **227:**474–483.
33. **Meier, O., and U. F. Greber.** 2004. Adenovirus endocytosis. J. Gene Med. **6**(Suppl. 1)**:**S152–S163.
34. **Mu, F. T., J. M. Callaghan, O. Steele-Mortimer, H. Stenmark, R. G. Parton, P. L. Campbell, J. McCluskey, J. P. Yeo, E. P. Tock, and B. H. Toh.** 1995. EEA1, an early endosome-associated protein. EEA1 is a conserved alpha-helical peripheral membrane protein flanked by cysteine "fingers" and contains a calmodulin-binding IQ motif. J. Biol. Chem. **270:**13503–13511.
35. **Okun, M. M., P. M. Day, H. L. Greenstone, F. P. Booy, D. R. Lowy, J. T. Schiller, and R. B. Roden.** 2001. L1 interaction domains of papillomavirus L2 necessary for viral genome encapsidation. J. Virol. **75:**4332–4342.
36. **Pastrana, D. V., R. Gambhira, C. B. Buck, Y. Y. Pang, C. D. Thompson, T. D. Culp, N. D. Christensen, D. R. Lowy, J. T. Schiller, and R. B. Roden.** 2005. Cross-neutralization of cutaneous and mucosal papillomavirus types with anti-sera to the amino terminus of L2. Virology **337:**365–372.
37. **Pisani, E., G. P. Garnett, N. C. Grassly, T. Brown, J. Stover, C. Hankins, N. Walker, and P. D. Ghys.** 2003. Back to basics in HIV prevention: focus on exposure. BMJ **326:**1384–1387.
38. **Pisani, E., S. Lazzari, N. Walker, and B. Schwartlander.** 2003. HIV surveillance: a global perspective. J. Acquir. Immune Defic. Syndr. **32**(Suppl. 1)**:** S3–S11.
39. **Pisani, P., D. M. Parkin, N. Munoz, and J. Ferlay.** 1997. Cancer and infection: estimates of the attributable fraction in 1990. Cancer Epidemiol. Biomarkers Prev. **6:**387–400.
40. **Pyeon, D., P. F. Lambert, and P. Ahlquist.** 2005. Production of infectious human papillomavirus independently of viral replication and epithelial cell differentiation. Proc. Natl. Acad. Sci. USA **102:**9311–9316.
41. **Richards, R. M., D. R. Lowy, J. T. Schiller, and P. M. Day.** 2006. Cleavage of the papillomavirus minor capsid protein, L2, at a furin consensus site is necessary for infection. Proc. Natl. Acad. Sci. USA **103:**1522–1527.

42. **Roden, R. B., E. M. Weissinger, D. W. Henderson, F. Booy, R. Kirnbauer, J. F. Mushinski, D. R. Lowy, and J. T. Schiller.** 1994. Neutralization of bovine papillomavirus by antibodies to L1 and L2 capsid proteins. J. Virol. **68:**7570–7574.
43. **Roden, R. B., W. H. Yutzy IV, R. Fallon, S. Inglis, D. R. Lowy, and J. T. Schiller.** 2000. Minor capsid protein of human genital papillomaviruses contains subdominant, cross-neutralizing epitopes. Virology **270:**254–257.
44. **Rohrer, J., A. Schweizer, D. Russell, and S. Kornfeld.** 1996. The targeting of Lamp1 to lysosomes is dependent on the spacing of its cytoplasmic tail tyrosine sorting motif relative to the membrane. J. Cell Biol. **132:**565–576.
45. **Sarver, N., M. S. Rabson, Y. C. Yang, J. C. Byrne, and P. M. Howley.** 1984. Localization and analysis of bovine papillomavirus type 1 transforming functions. J. Virol. **52:**377–388.
46. **Selinka, H. C., T. Giroglou, T. Nowak, N. D. Christensen, and M. Sapp.** 2003. Further evidence that papillomavirus capsids exist in two distinct conformations. J. Virol. **77:**12961–12967.
47. **Selinka, H. C., T. Giroglou, and M. Sapp.** 2002. Analysis of the infectious entry pathway of human papillomavirus type 33 pseudovirions. Virology **299:**279–287.
48. **Slupetzky, K., R. Gambhira, T. D. Culp, S. Shafti-Keramat, C. Schellenbacher, N. D. Christensen, R. B. Roden, and R. Kirnbauer.** 2006. A papillomavirus-like particle (VLP) vaccine displaying HPV16 L2 epitopes induces cross-neutralizing antibodies to HPV11. Vaccine **25:**2001–2010.
49. **Trus, B. L., R. B. Roden, H. L. Greenstone, M. Vrhel, J. T. Schiller, and F. P. Booy.** 1997. Novel structural features of bovine papillomavirus capsid revealed by a three-dimensional reconstruction to 9 A resolution. Nat. Struct. Biol. **4:**413–420.
50. **Unckell, F., R. E. Streeck, and M. Sapp.** 1997. Generation and neutralization of pseudovirions of human papillomavirus type 33. J. Virol. **71:**2934–2939.
51. **Volpers, C., F. Unckell, P. Schirmacher, R. E. Streeck, and M. Sapp.** 1995. Binding and internalization of human papillomavirus type 33 virus-like particles by eukaryotic cells. J. Virol. **69:**3258–3264.
52. **Yang, R., P. M. Day, W. H. Yutzy IV, K. Y. Lin, C. F. Hung, and R. B. Roden.** 2003. Cell surface-binding motifs of L2 that facilitate papillomavirus infection. J. Virol. **77:**3531–3541.
53. **Zhou, J., D. J. Stenzel, X. Y. Sun, and I. H. Frazer.** 1993. Synthesis and assembly of infectious bovine papillomavirus particles in vitro. J Gen. Virol. **74:**763–768.